Ultrasonic based concrete defects identification via wavelet packet transform and GA-BP neural network

Tianyu Hu [Equal first author, 1] , **Jinhui Zhao** [Corresp., Equal first author, 2] , **Ruifang Zheng** [1] , **Pengfeng Wang** [3] , **Xiaolu Li** [1] , **Qichun Zhang** [4]

[1] College of Mechanical and Electrical Engineering, China Jiliang University, Hangzhou, China

[2] Key laboratory for technology in rural water management of Zhejiang province, College of Electrical Engineering,, Zhejiang University of Water Resources and Electric Power, Hangzhou, China

[3] College of Modern Science and Technology, China Jiliang Univercity, Hangzhou, China

[4] Department of Computer Science, University of Bradford, Bradford, United Kingdom

Corresponding Author: Jinhui Zhao
Email address: jhzhao2009@zju.edu.cn

Concrete is the main material in building. Since its poor structural integrity may cause accidents, it is significant to detect defects in concrete. However, it is a challenging topic as the unevenness of concrete would lead to the complex dynamics with uncertainties in the ultrasonic diagnosis of defects. Note that the detection results mainly depend on the direct parameters, e.g. the time of travel through the concrete. The current diagnosis accuracy and intelligence level are difficult to meet the design requirement for automatic and increasingly high-performance demands. To solve the mentioned problems, our contribution of this paper can be summarized as establishing a diagnosis model based on the GA-BPNN method and ultrasonic information extracted that helps engineers identify concrete defects. Potentially, the application of this model helps to improve the working efficiency, diagnostic accuracy and automation level of ultrasonic testing instruments. In particular, we propose a simple and effective signal recognition method for small-size concrete hole defects. This method can be divided into two parts: 1) signal effective information extraction based on wavelet packet transform (WPT), where mean value, standard deviation, kurtosis coefficient, skewness coefficient and energy ratio are utilized as features to characterize the detection signals based on the analysis of the main frequency node of the signals, and 2) defect signal recognition based on GA optimized back propagation neural network (GA-BPNN), where the cross-validation method has been used for the stochastic division of the signal dataset and it leads to the BPNN recognition model with small bias. Finally, we implement this method on 150 detection signal data which are obtained by the ultrasonic testing system with 50kHz working frequency. The experimental test block is a C30 class concrete block with 5mm, 7mm, and 9mm penetrating holes. The information of the experimental environment, algorithmic parameters setting and signal processing procedure are described in detail. The average

recognition accuracy is 91.33% for the identification of small size concrete defects according to experimental results, which verifies the feasibility and efficiency.

Ultrasonic based Concrete Defects Identification via Wavelet Packet Transform and GA-BP Neural Network

Tianyu Hu[*,1], Jinhui Zhao [*,2], Ruifang Zheng [1], Pengfeng Wang [3], Xiaolu Li [1] and Qichun Zhang [4]

[1] College of Mechanical and Electrical Engineering, China Jiliang University, Hangzhou, Zhejiang Province, China

[2] Key laboratory for technology in rural water management of Zhejiang province, College of Electrical Engineering, Zhejiang University of Water Resources and Electric Power, Hangzhou Zhejiang Province, China

[3] College of Modern Science and Technology, China Jiliang University, Hangzhou, Zhejiang Province, China

[4] Department of Computer Science, University of Bradford, Bradford, BD7 1DP, the United Kingdom

* These authors contributed to the work equally and should be regarded as co-first authors.

Corresponding Author: Jinhui Zhao

No. 583, Xuelin Street, Jianggan District, Hangzhou, Zhejiang Province 310018, China

Email address: jhzhao2009@zju.edu.cn

ABSTRACT

Concrete is the main material in building. Since its poor structural integrity may cause accidents, it is significant to detect defects in concrete. However, it is a challenging topic as the unevenness of concrete would lead to the complex dynamics with uncertainties in the ultrasonic diagnosis of defects. Note that the detection results mainly depend on the direct parameters, e.g. the time of travel through the concrete. The current diagnosis accuracy and intelligence level are difficult to meet the design requirement for automatic and increasingly high-performance demands. To solve the mentioned problems, our contribution of this paper can be summarized as establishing a diagnosis model based on the GA-BPNN method and ultrasonic information extracted that helps engineers identify concrete defects. Potentially, the application of this model helps to improve the working efficiency, diagnostic accuracy and automation level of ultrasonic testing instruments. In particular, we propose a simple and effective signal recognition method for small-size concrete hole defects. This method can be divided into two parts: 1) signal effective information extraction based on wavelet packet transform (WPT), where mean value, standard deviation, kurtosis coefficient, skewness coefficient and energy ratio are utilized as features to characterize the detection signals based on the analysis of the main frequency node of the signals, and 2) defect signal recognition based on GA optimized back propagation neural network (GA-BPNN), where the cross-validation method has been used for the stochastic division of the signal dataset and it

40 leads to the BPNN recognition model with small bias. Finally, we implement this method on 150
41 detection signal data which are obtained by the ultrasonic testing system with 50kHz working
42 frequency. The experimental test block is a C30 class concrete block with 5mm, 7mm, and 9mm
43 penetrating holes. The information of the experimental environment, algorithmic parameters
44 setting and signal processing procedure are described in detail. The average recognition accuracy
45 is 91.33% for the identification of small size concrete defects according to experimental results,
46 which verifies the feasibility and efficiency.

47 **INTRODUCTION**

48 Concrete materials are widely used in modern buildings. It is a non-uniform material mixed with
49 cement, sand, gravel and water. The random distributions of coarse aggregate and cement mortar
50 are the causes of the heterogeneity of concrete. There exist various forms of deterioration and
51 defects of concrete structures because of aging and environmental damage, such as internal voids
52 (Bien, Kaminski & Kuzawa,2019). Among the main health problems of concrete, surface defects
53 are relatively easy to be detected. However, internal defects are hidden in the concrete, which is
54 difficult to detect and is more harmful. It is significant to detect and analyze the internal defects of
55 concrete structures in time to avoid the potential related accidents.

56 Commonly used methods of non-destructive testing include electromagnetic, radiological and
57 ultrasound (Schabowicz, 2019). Ultrasonic has the advantages of strong penetrating power and
58 high sensitivity, so it is mostly used in material defect detection (Janku, et al., 2019). In actual
59 inspection tasks, ultrasonic detection of concrete defects is based on the observation of acoustic
60 parameters, propagation time, amplitude and main frequency of ultrasonic detection signals, etc.
61 (Ushakov, Davydov, 2013; Ozsoy, Koyunlu & Ugweje, 2017). For example, NDT James V-C-400
62 V-Meter MK IV still uses the ultrasonic pulse velocity method to characterize the detection signal.
63 These applied methods are susceptible to individual subjective factors and experience levels.

64 The applications of modern signal processing and artificial intelligence algorithms can achieve the
65 automatic recognition of signals and also improve recognition efficiency and accuracy (Tibaduiza-
66 Burgos & Torres-Arredondo, 2015; Javed et al., 2020). It is necessary to obtain effective
67 information to characterize different types of signals before performing detection signal
68 recognition. At present, many methods have been used to find the effective features of complex
69 signals (Cheema & Singh, 2019). These signal analysis methods are mainly sparse representation,
70 Hilbert-Huang transform, Fourier transform, wavelet transform, and so on (Liu et al., 2021; Kumar
71 & Kumar, 2019; Bochud et al., 2015; Rodriguesa et al., 2019). However, it is difficult to extract
72 the key information from concrete ultrasonic detection signals due to the noise influence and many
73 mutational components, such as mutational amplitude (Cheema & Singh 2019; Combet, Gelman,
74 & LaPayne, 2012). Among these signal preprocessing methods, wavelet transform can effectively
75 deal with the non-stationary and high-noise complex signals. This method has been applied to
76 process ultrasonic signals (Acciani et al.,2010).

77 Machine learning models are established with simple structures which are suitable for small
78 sample dataset, while the scholars often choose these methods to identify detection signals (Iyer
79 et al., 2012). For now, commonly used machine learning algorithms include support vector

80 machine, neural network, etc. (Rajput et al., 2021; Xu & Jin, 2018). As a class of neural networks,
81 BP neural network (BPNN) is a classic model. It has strong nonlinear mapping ability and simple
82 structure (Wang, 2015). After optimization by genetic algorithm, the fitting ability and running
83 speed can be improved. Note that BPNN is widely used in the field of pattern recognition, where
84 deep learning is one of the most popular methods in pattern recognition. In the field of ultrasonic
85 inspection, deep learning has been used to identify inspection images (Slonski, Schabowicz, &
86 Krawczyk, 2020). However, deep learning was rarely used to recognize concrete ultrasonic
87 detection signals due to the high hardware performance requirements (Shrestha & Mahmood,
88 2019).
89 Saechai S. et al. (Saechai, Kongprawechnon & Sahamitmongkol, 2012) used the support vector
90 machine to identify the defect detection signals of concrete which obtained higher recognition
91 accuracy. Chen Y. et al. (Chen & Ma, 2011) extracted features of the weld detection signal by
92 wavelet packet transform and used radial basis function neural network to recognize defects.
93 Zhang K.X. et al. (Zhang et al., 2020) used genetic algorithm-back propagation neural network to
94 evaluate the laser ultrasonic fault signals of uniform metal structures. The composition of the
95 concrete selected in our paper is more complex than the research objects in the literatures. When
96 these methods are used directly to identify concrete detection signals, the performance would be
97 deteriorated. Therefore, a novel ultrasonic-based solution should be developed for concrete defect
98 detection.
99 In this paper, we propose an intelligent method to process the ultrasonic lateral detection signals
100 of penetrating holes in concrete. The main contributions and objective are summarized as follows:
101 •   To improve the performance of more effective calculation and high identification accuracy,
102   the ultrasonic detection signals are decomposed by WPT in order to extract the useful
103   information in the detection signal. As a result, we extract the 5 effective features of the
104   processed signal.
105 •   Genetic algorithm has been used to optimize the structural parameters of the BP neural
106   network. In the experiments with measured data, the average classification accuracy of GA-
107   BPNN is increased by 4.66%, 4%, and 5.33% compared with BPNN, SVM, and RBF,
108   respectively.
109 •   This paper presents a generalized research framework on the processing and recognition of
110   concrete ultrasonic detection signals, which lays the technical foundation for achieving the
111   intelligent and automatic detection of concrete.
112 The rest of the paper has been organized as follows: In section 2, we describe the whole algorithmic
113 procedure and principles briefly. And we present the experimental system and algorithmic
114 parameters setting in the 3rd section. The test results and analysis are presented in the 4th section.
115 We draw a conclusion in the 5th section.

116 **THE PROCESS OF THE PROPOSED ALGORITHM**

117 The ultrasonic pulse velocity (UPV) method is widely used in ultrasonic testing instruments which
118 cannot meet the needs of small-size concrete defect detection. The levels of intelligence and
119 automation of concrete testing instruments need to be improved urgently. To solve this problem,

120 we propose a method based on WPT and GA-BPNN. In particular, the presented algorithm in this
121 paper consists of three parts. First, wavelet packet transform is used to attenuate noise and retain
122 effective information from the non-stationary concrete ultrasonic detection signals. Then, the
123 features of processed signals are extracted as the feature vector. Finally, we use the BPNN
124 optimized by the improved GA to identify the detection signals and the K-fold cross-validation is
125 introduced to verify the stability and generalization of GA-BPNN. We describe the main steps in
126 the following subsections.

127 **Wavelet packet transform**

128 Wavelet transform is a multi-resolution analysis method (Babouri et al., 2019), which is a process
129 of using wavelet basis functions to decompose a signal into components of different frequency
130 bands, processing the wavelet packet coefficients, and reconstructing these components into a
131 complete signal (Kim et al., 2020). When using the wavelet transform to process a non-stationary
132 signal, there are different resolutions at different locations. WPT can accurately obtain the high
133 and low-frequency components of the signal (Schimmack & Mercorelli, 2018). Therefore, WPT
134 can be considered as an effective pre-processing algorithm for feature extraction. However, the
135 wavelet transform cannot extract the detailed information of detection signals.

136 ***Decomposition and reconstruction of WPT***

137 The structure diagram of the three-layer decomposition of wavelet packet is given in Fig. 1.

138 In Fig. 1, S means an original signal. Then, S can be decomposed according to the equation (1) to
139 obtain A and D. A is a low-frequency component and D is a high-frequency component after each
140 decomposition of an original signal. Continuously, we decompose A and D in the same way.
141 Finally, S is decomposed into eight components at different frequency bands.

142 The basic calculation formulas of WPT are shown in equations (1-2).

$$\begin{cases} d_j^{2n}[k] = \sum_{l \in Z} h_{l-2k} d_{j+1}^n[l] \\ d_j^{2n+1}[k] = \sum_{l \in Z} g_{l-2k} d_{j+1}^n[l] \end{cases} \tag{1}$$

$$d_j^{2n+1}[k] = \sum_{l \in Z} h_{k-2l} d_j^{2n}[l] + \sum_{l \in Z} g_{k-2l} d_j^{2n+1}[l] \tag{2}$$

143 where d_{j+1}^n represents a wavelet packet coefficient sequence of the signal to be decomposed, j
144 represents a scale factor, n represents the number of frequency bands, k and l are the positions of
145 coefficients sequences, d_j^{2n} and d_j^{2n+1} represent wavelet packet coefficients sequences of signals
146 after decomposition, ***h*** represents orthogonal real coefficients matrices of low-pass filters, and ***g***
147 represents orthogonal real coefficients matrices of high-pass filters.

148 We use the cost function to select the wavelet packet basis for the signal decomposition. At present,
149 the Shannon entropy (Shi et al., 2021) is widely used where the entropy of the wavelet packet
150 coefficient sequence ***d***=$\{d_j\}$ is defined by equation (3).

$$M(d) = -\sum_j P_j \log_2 P_j \tag{3}$$

151 where $P_j = \dfrac{|d_j|^2}{\|d\|^2}$, and when $P=0$, $P\log_2 P=0$.

152 *Wavelet basis function selection*

153 How to choose the appropriate wavelet basis function is vital besides WPT decomposes ultrasonic
154 detection signals precisely. Samaratunga D. et al. (Samaratunga, Jha & Gopalakrishnan, 2016)
155 think the time-frequency change of non-stationary signal is well represented by the Daubechies
156 wavelet function in the time-frequency domain. In this paper, the db15 wavelet is selected as the
157 base function of WPT according to the decomposition experiment analysis.

158 **Ultrasonic signal features selection**

159 In pattern recognition, feature extraction is normally used for two processes: object feature data
160 collection and classification. The quality and property of feature data greatly affect the design and
161 the performance of pattern recognition classifiers, e.g., monotonicity, which is a key problem of
162 pattern recognition.

163 Scholars used wavelet coefficients after wavelet transform as feature vectors, which resulted in the
164 very high-dimensional input data of the recognition model (Cruz et al., 2016). Wan P. et al. (Wan
165 & Li, 2014) only extracted one type of feature including the energy ratio of each node after wavelet
166 packet decomposition as the feature vector of identifying defects in carbon-fiber-reinforced
167 polymer. Wang X.K. et al. (Wang et al., 2019) selected 9 features including the average peak
168 spacing, dominant frequency, etc., to identify weld quality defects. Furthermore, scholars also
169 choose features such as mean value, standard deviation, kurtosis, etc. as the inputs of ultrasonic
170 detection signal recognition models (Virmani et al, 2017).

171 Based on commonly used features in the field of ultrasonic testing, we have selected useful and
172 non-redundant features by analyzing the calculation formulas of the features and conducting
173 experimental tests. For example, the calculation formulas and physical meaning of mean square
174 value and energy are very similar, and they are not used as features collectively. Finally, the five
175 features of mean value, standard deviation, kurtosis coefficient, skewness coefficient and energy
176 ratio are retained (Wan & Li, 2014; Zhang, Duffy & Orlandi, 2017).

177 In order to make the feature values in the same order of magnitude and improve the convergence
178 speed of the model, we normalize the extracted features (Bagan et al., 2009). The five feature
179 values are mapped to [-1,1] and the normalized feature values are taken as input variables of the
180 BPNN model in this paper.

181 **GA-BP neural network (GA-BPNN)**

182 *BP Neural Network (BPNN)*

183 A BPNN is made up of an input layer, a hidden layer, and an output layer. The input signal of
184 BPNN propagates forward, and the error propagates backward. It can approximate the function of
185 finite discontinuities (Wang, 2015). In addition, it has a powerful ability to deal with nonlinear
186 problems. The structure is shown in Fig. 2.

187 In Fig. 2, x is input data, ω_{ij} is the weight between the input layer i and the hidden layer j, α is
188 biases of the hidden layer, f_1 is activation functions used for the hidden layer, ω_{jk} is the weight
189 between the hidden layer j and the output layer k, β is biases of the output layer, f_2 is the activation
190 function used for the output layer, and y is the output of the network.

191 *Genetic algorithm (GA)*

192 The outputs of the BPNN are calculated according to its input-output function built on the
193 generated weights, biases and number of hidden nodes. In this paper, the improved GA (Peng et
194 al., 2013) has been used to optimize initial weights, biases and the number of hidden layer nodes.
195 This method can make BPNN convergent fast with higher precision (Han & Huang, 2019).
196 According to the description of the improved GA (Peng et al., 2013), we use binary to code
197 variables of the number of hidden layer node and use real numbers to code variables of the
198 corresponding weights and biases for building candidate solutions in GA. We assume the
199 maximum number of hidden layer node in the BPNN is l, and the number of input and output layer
200 nodes in the network are n and m, respectively. Then the total number of optimization variables is
201 $1+(l \cdot n)+l+(l \cdot m)+m$. The coding of all parameters in a candidate solution is shown in Fig. 3. For
202 instance, if the number of hidden layer nodes is represented by a q-bit 0 to 1 string, the range of
203 the number of hidden layer node is 0 to 2^q-1, and $l = 2^q$-1.
204 In Fig. 3, q is the number of candidates hidden layer node, l is the maximum number of hidden
205 layer node, $0 < q \leqslant l$, n is the number of nodes in the input layer, m is the number of nodes in the
206 output layer. Furthermore, errors between the actual values and the output values of the BPNN are
207 calculated, then the reciprocal of the sum of squared errors is used as the fitness function in the
208 GA.
209 In this paper, the roulette wheel method is used as the selection operator. Two individuals are
210 selected by the selection operator. Then we use the one-point crossover method to process the
211 binary coding arrays. The arithmetic crossover operator is used for the real number encoding
212 sequences. For binary coding arrays, the simple mutation operator is used. We apply the non-
213 uniform mutation operator to the real coding sequences in this paper. Briefly, we first encode the
214 variables that need to be optimized; next, the fitness values in the initial population are calculated;
215 then, we perform selection, crossover, and mutation operations to generate a new generation of
216 population and obtain the maximum fitness value of each generation; finally, the optimal variable
217 values are obtained by decoding the individual with the largest fitness value among all offspring.
218 **Overall steps of the WPT and GA-BPNN method**
219 To describe the proposed concrete ultrasonic detection signal identification method, the main steps
220 are summarized as follows.
221 Step1: The ultrasonic detection signal is decomposed into three layers by WPT sub-algorithm, and
222 the wavelet packet coefficients in the main frequency node are extracted to reconstruct the signal;
223 Step2: The five feature variables of the reconstructed signals are calculated to establish the feature
224 dataset;
225 Step3: Adopt K-fold cross-verification method to divide the dataset;
226 Step4: The genetic algorithm is executed to calculate the optimal configuration parameter of
227 BPNN; select the optimal parameters of BPNN from the optimal solutions of GA, then obtain an
228 optimized BPNN;
229 Step5: Use the test dataset to test the BPNN, output the recognition results.
230 The flowchart of the proposed method is given in Fig.4.
231 **EXPERIMENTAL ENVIRONMENT AND TEST**

232 **Experimental set-up and dataset**

233 As an engineering application, we apply the ultrasonic transmission detection method to the
234 practical ultrasonic detection system in which we use the P28F ultrasonic probes with the 50kHz
235 working frequency to generate the ultrasonic signals. An ± 80-Volt square wave pulse signal is
236 generated at the transmitting end to excite the ultrasonic probe vibration. The signal sampling
237 frequency of the receiving end is 1MHz. The analog-to-digital conversion module used for data
238 acquisition is 12 bits. Each detection signal used in this paper contains a total of 18,000 sampling
239 points in 6 cycles. The Fig. 6 is concrete test sample. Concrete is mainly composed of cement,
240 sand, coarse aggregate and water, the material ratio of C30 class concrete is 461, 175, 512 and
241 1252 kg/m^3. The size of the sample block is pre-specified as follows: the length is 30cm, the width
242 is 20cm and the height is 20cm.

243 The experimental data are obtained by sampling repeatedly at the different positions shown in Fig.
244 7. The white dots of test points shown in Fig. 7 are all measured evenly. Hole defects are available
245 in three sizes. The distance between two penetrating holes is 85 mm. The diameters of penetrating
246 holes are 5mm,7mm and 9mm, respectively. Three test points are placed on the surface of each
247 kind of hole defect. Six test points of the defect-free structure are located between the points over
248 the holes. The horizontal and vertical distances between the detection positions are both 45mm.
249 Fifteen detection positions are arranged on the concrete surface, and 10 detection data signals are
250 obtained for each detection point. In this case study, a total of 150 ultrasonic transmission detection
251 data samples are obtained through the experimental device in Fig. 8, including 60 sample data
252 signals from the non-defective structure, and 90 sample data signals from the defective structure.
253 Fig. 5 shows the experimental data acquisition process of the detection system.

254 **Algorithm parameter settings**

255 According to the wavelet basis function selection rule and the distribution of these detection
256 signals' time-frequency characteristics, the db15 wavelet function is selected to perform the three-
257 layer WPT. And most of the valid information of the signal is included in the first node of the third
258 layer after decomposing the detection signals.

259 In algorithm experiments, our computer is 64-bit Windows operation system. The hardware
260 configuration includes 2.08 GHz CPU, Inter Core i5-8400 with 6 cores, and 32GB 2400MHz
261 DDR4 memory. The application software is MATLAB R2014a version. The main parameter
262 setting of the proposed algorithm is given as follows.

263 The WPT parameters setting is: the wavelet basis function is db15, the number of decomposition
264 levels is 3, and the optimal wavelet basis Shannon entropy is selected.

265 The GA algorithmic parameters setting is: the maximum genetic algebra g is 100, the population
266 size p is 50, the binary code length q is 5, the crossover probability Pc is 0.7, and the mutation
267 probability Pm is 0.05.

268 The BPNN algorithmic parameters setting is: the number of input nodes is 5, the number of output
269 nodes is 2, the training stop condition is that the model error reaches 0.001 or the epochs of training
270 reaches 1000, and the learning rate is 0.01. Simultaneously, the cross-validation is used for training
271 and testing the GA-BPNN model. The hidden layer function used in this paper is the hyperbolic

272 tangent sigmoid transfer function (tansig), and the output layer function is the Log-sigmoid transfer
273 function (logsig).
274 The parameters setting of the K-fold cross-validation is: K=3, N=150. That is, 150 samples of
275 experimental data are randomly divided into 3 groups, and 2 groups are selected as the training
276 data of the GA-BPNN in turn, and the remaining 1 group is used as the testing data. So, the
277 recognition rate of each test is recorded and the final result is the average of 3 recognition rates.

278 **Results & Discussion**

279 **Experimental data analysis**
280 Four typical waveform samples of raw detection signals are randomly selected from the
281 experimental data, and their last period data are drawn in Fig. 9
282 The figure shows the similarities and differences of the ultrasonic propagating in the concrete test
283 block. Based on the physical mechanism of the ultrasonic propagation, the different diameters of
284 holes are the main reason for the difference between ultrasonic detection signal waveforms. In
285 addition, the sizes and the shapes of gravel at different locations are different in the concrete, which
286 is another important reason for the different detection waveforms (Garnier et al., 2009).
287 Based on the reconstructed data, five features extracted from 150 signals are calculated. The five
288 features are separately shown in Figs. 10-14.
289 Five features of the reconstructed defective and defect-free signals do not show obvious regularity
290 or organization from Figs. 10-14. The figures show that the feature values are different more or
291 less even they are extracted from the same defect shared the same diameters of penetrating holes,
292 or at the same detection points. Five features are aliasing and these reconstructed signals are
293 inseparable linearly based on the mere measurement of single feature. On the one hand, the uneven
294 distribution of coarse aggregate in concrete will generate acoustic measurement uncertainty, and
295 that causes the complexity of ultrasonic detection signal. In particular, it is a non-linear, non-
296 stationary signal and contains many mutational components. On the other hand, the stability and
297 accuracy of the hardware system influence the output deviation, so the detection signals exist a
298 certain distortion inevitably. Nevertheless, it can be seen that partial feature data are distributed
299 centrally, such as the kurtosis coefficient of 9 mm defect detection data in Fig. 12. Although
300 Different detection signals have similarities on a single feature, we can distinguish differences
301 between different signals on multiple features fusion. Then, five features are regarded as essential
302 characteristics for the classification of defects in this paper.

303 **Comparison**
304 The optimal solution is used to initialize the configuration parameters for the proposed GA-BPNN
305 algorithm. The optimal number of hidden layer nodes of BPNN calculated by GA with the three-
306 fold cross-validation method is 12, and then the number of each layer's nodes is 5, 12, and 2.
307 To demonstrate the advantages and disadvantages of the GA-BPNN, a BPNN without optimization
308 is utilized for algorithmic performance analysis, and we further draw their convergent curves. We
309 use a default function in the neural network toolbox to initialize weights and biases, with 11 hidden
310 layer nodes, according to the empirical rule (2*5+1) in the paper of Guo Z.H. et al. (Guo et al.,
311 2011). Some parameters of the BPNN include the number of input nodes, the number of output

312   nodes, the training stop condition, learning rate and activating function are the same as the
313   parameters setting of GA-BPNN in Section 3.
314   The training error curves and test error curves of the computational processes are painted in Figs.
315   15-16, where two figures show how the outputs of models converge to the actual tag value. The
316   feature data picked up for operating and drawing the curves are randomly selected from the training
317   dataset and the test dataset respectively. The error set by the BPNN in this paper is 0.001, and the
318   epochs required by BPNN are more than twice that of GA-BPNN. The computational cost of the
319   BPNN is higher than that of GA-BPNN. In addition, the GA-BPNN also converges faster in the
320   early stage of operation. In Figs. 15-16, it can be seen from the mean squared error curves that the
321   GA-BPNN takes fewer epochs under the same termination conditions. The GA-BPNN has higher
322   operating efficiency and convergence speed to approach the model's predictive values. The
323   statistical results on 100 training data calculated by GA-BPNN with the three-fold cross-validation
324   are shown in Table 1, the statistical results on the 50 test data are shown in Table 2.
325   Although the convergence speed of GA-BPNN is higher, it has to spend much time to solve the
326   optimum in the training stage, i.e., it is about 489.049 seconds to search the optimum. Its average
327   training time is about 0.0993 seconds and the average test time is about 0.0053 seconds.
328   Correspondingly, the average training time of BPNN is about 0.1413 seconds and its average test
329   time is about 0.0057 seconds. Its test recognition accuracy is about 86.67% which is less than the
330   recognition accuracy of GA- BPNN.
331   Three defect recognition accuracies from the three-fold cross-validation are all higher than 90%
332   shown in the statistical results, which can prove the extracted features are effective in
333   characterizing the presence or absence of defects in concrete, and the GA-BPNN is feasible as a
334   concrete defect-recognition model. Furthermore, the proposed method can identify the defects
335   automatically from detection data, then operators do not need to possess professional detection
336   knowledge for reading and identifying recognition results. It is quite important for its practical
337   engineering applications.
338   According to previous research on the recognition method of concrete ultrasonic detection signal,
339   we choose radial basis function network (RBF) (Chen & Ma, 2011) and support vector machine
340   (SVM) (Saechai, Kongprawechnon & Sahamitmongkol, 2012) using the data in this paper to carry
341   out classification experiments. Also, under the 3-fold cross-validation, 150 concrete ultrasonic data
342   consisting of 5 features are used. The results of the comparative experiment are shown in Table 3.
343   The recognition accuracy of SVM, RBF, and BPNN methods have little differences, but none of
344   them reaches 90%. Compared with previous studies, the size of the concrete defects in this paper
345   are smaller and therefore the detection signal is more challenging to be identified. The method we
346   proposed is more accurate than the above three methods.
347   It is shown that the proposed method leads to the performance approaching high recognition
348   accuracy. When measuring the acoustic, the degree of adhesion and contact force of the ultrasonic
349   probe to the concrete surface may cause the recognition error due to the fact that concrete is a
350   complex and multi-phase medium. Therefore, the obtained detection signals are complex and

351   diverse. Although it is hard to completely identify all modes of the complex ultrasonic detection
352   signals from concrete, more defect-type will be further investigated as our future works.

Conclusions and future work

354   In order to recognize the concrete defects with high reliability and accuracy by using ultrasonic
355   testing signals, we propose an intelligent method which includes a signal processing sub-algorithm
356   and a recognition sub-algorithm. We extract fundamental information from the first node of the
357   third layer by using wavelet packet transform (WPT) and calculate five feature variables of the
358   reconstructed signals. Moreover, the GA-BPNN-based sub-algorithm identifies the concrete
359   defects, where GA optimized BP neural network (GA-BPNN) model has been proposed
360   embedding a K-fold cross-validation method. As a practical application of a typical type of hole
361   defects in concrete, we utilize the method to identify the defects in a C30 class concrete test block.
362   Based upon the test points, we obtained 150 ultrasonic detection signals containing no defect and
363   hole defects at various locations, and then performed identification experiments based on these
364   data sets using the method in this paper. GA-BPNN has higher diagnosis accuracy and faster
365   running speed than existing methods. The experimental results show the effectiveness of the
366   proposed method while the concrete hole defects have been recognized with high accuracy.
367   In the future, we will further verify the effectiveness of this method in more types of concrete
368   defect (e.g., cracks and foreign matter) ultrasonic detection signal data and develop more effective
369   methods to solve complex problems in the field (Mittal et al., 2020.), such as characteristic indexes,
370   optimizer, machine learning. Then these effective methods will be extended to more detection
371   signal fields. Simultaneously, the sensor network solution is also our future directly for information
372   fusion (Naeem et al.,2021). Simultaneously, the uneven distribution of coarse aggregate could be
373   considered as a stochastic distribution optimization problem (Ren, Zhang & Zhang, 2019), its
374   influence on the accuracy of detection signal recognition is another theoretical perspective for our
375   future works.

Acknowledgements

377   We thank two units for their help in designing the hardware system and the actual parameters
378   testing of the ultrasonic probe, Hangzhou Ruidian Meter Co., Ltd. and Shanghai Ultra Precision
379   Motion Control and Detection Engineering Research Center.

References

381   **Bien J, Kaminski T, Kuzawa M. 2019.** Taxonomy of non-destructive field tests of bridge
382   materials and structures. *Archives of Civil and Mechanical Engineering* **19**:1353-1367.
383   **Schabowicz K. 2019.** Non-destructive testing of materials in civil engineering. *Material* **12**:3237.
384   **Janku M, Cikrle P, Grosek J, Anton O, Stryk J. 2019.** Comparison of infrared thermography,
385   ground-penetrating radar and ultrasonic pulse echo for detecting delaminations in concrete
386   bridges. *Construction and Building Materials* **225**:1098-1111.
387   **Ushakov VM, Davydov DM. 2013.** A review of international (ISO) and European (EN) standards
388   for the ultrasonic testing of welded joints. *Russian Journal of Nondestructive Testing* **49**:61-
389   66.

390   **Ozsoy U, Koyunlu G, Ugweje OC. 2017.** Nondestructive Testing of Concrete using Ultrasonic
391   Wave Propagation. *In Proceedings of 13th International Conference on Electronics, Computer*
392   *and Computation (ICECCO)*, Abuja, Nigeria, 28-29.
393   **Tibaduiza-Burgos DA, Torres-Arredondo MA. 2015.** Investigation of an expert health
394   monitoring system for aeronautical structures based on pattern recognition and acousto-
395   ultrasonics. *Smart Materials and Structures* **24**:1-18.
396   **Cheema A, Singh M. 2019.** Psychological stress detection using phonocardiography signal: An
397   empirical mode decomposition approach. *Biomedical Signal Processing and Control* **49**:493-
398   505.
399   **Combet F, Gelman L, LaPayne G. 2012.** Novel detection of local tooth damage in gears by the
400   wavelet bicoherence. *Mechanical Systems and Signal Processing* **26**:218-228.
401   **Zhu Q, Wang YS, Shen GQ. 2011.** Comparison and application of time-frequency analysis
402   methods for nonstationary signal processing. *Advanced Research on Computer Education,*
403   *Simulation and Modeling*, PTI **175**:286-291.
404   **Liu SY, Li ZP, Wu T, Zhang W. 2021.** Determining ultrasound arrival time by HHT and kurtosis
405   in wind speed measurement. *Electronics* **10**:523.
406   **Kumar A, Kumar R. 2019.** Role of Signal Processing, Modeling and decision making in the
407   diagnosis of rolling element bearing defect: a review. *Journal of Nondestructive Evaluation*
408   **38**:5.
409   **Bochud N, Gomez AM, Rus G, Peinado AM. 2015.** A sparse digital signal model for ultrasonic
410   nondestructive evaluation of layered materials. *Ultrasonics* **62**:169-173.
411   **Iyer S, Sinha SK, Tittmann BR, Pedrick MK. 2012.** Ultrasonic signal processing methods for
412   detection of defects in concrete pipes. *Automation in Construction* **22**:135-148.
413   **Naeem A, Abdul RJ, Muhammad R, Sidra A, Jerry CWL, & Thippa RG. 2021.** DARE-SEP:
414   A hybrid approach of distance aware residual energy-efficient SEP for WSN. *IEEE*
415   *Transactions on Green Communications and Networking* 5(2):611-621.
416   **Rajput DS, Basha SM, Xin Q, Gadekallu TR, Kaluri R, Lakshmanna K, Maddikunta PKR.**
417   **2021.** Providing diagnosis on diabetes using cloud computing environment to the people living
418   in rural areas of India. *Journal of Ambient Intelligence Humanized Computing* doi:
419   10.1007/s12652-021-03154-4.
420   **Xu YD, Jin RY. 2018.** Measurement of reinforcement corrosion in concrete adopting ultrasonic
421   tests and artificial neural network. *Construction and Building Materials* **177**:125-133.
422   **Acciani G, Brunetti G, Fornarelli G, Giaquinto A. 2010.** Angular and axial evaluation of
423   superficial defects on non-accessible pipes by wavelet transform and neural network-based
424   classification. *Ultrasonics* **50**:13-25.
425   **Rodriguesa LFM, Cruzb FC, Oliveirac MA, Simas EF, Albuquerqued MCS, Silvad IC,**
426   **Fariasd CTT. 2019.** Carburization level identification in industrial HP pipes using ultrasonic
427   evaluation and machine learning. *Ultrasonics* **94**:145-151.
428   **Saechai S, Kongprawechnon W, Sahamitmongkol R. 2012.** Test system for defect detection in
429   construction materials with ultrasonic waves by support vector machine and neural network.

430 *In Proceedings of 6th International Conference on Soft Computing and Intelligent Systems*
431 *(SCIS)*, Kobe, Japan, 20-22, November, pp.1034-1039.

432 **Chen Y, Ma HW. 2011.** Application of artificial neural network to flaw classification in ultrasonic
433 testing. *Advanced Materials Research* **328**:1876-1880.

434 **Zhang KX, Lv GL, Guo SF, Chen D, Liu YJ, Feng W. 2020.** Evaluation of subsurface defects
435 in metallic structures using laser ultrasonic technique and genetic algorithm-back propaga-tion
436 neural network. *NDT & E International* **116**:102339.

437 **Shrestha A, Mahmood A. 2019.** Review of deep learning algorithms and architectures. *IEEE*
438 *Access* **7**:53040-53065.

439 **Wang XP. 2015.** Research and optimization of BP neural network algorithm. *In Proceedings of*
440 *2015 Seventh International Conference on Measuring Technology and Mechatronics*
441 *Automation (ICMTMA 2015)*, Nanchang, China, 13-14 June, pp.818-822.

442 **Slonski M, Schabowicz K, Krawczyk E. 2020.** Detection of flaws in concrete using ultrasonic
443 tomography and convolutional neural networks. *Materials* **13**:1557.

444 **Babouri MK, Ouelaa N, Kebabsa T, Djebala A. 2019.** Application of the cyclostationarity
445 analysis in the detection of mechanical defects: comparative study. *International Journal of*
446 *Advanced Manufacturing Technology* **103**:1681-1699.

447 **Kim HJ, Mission JL, Dinoy PR, Kim HS, Park TW. 2020.** Guidelines for impact echo test
448 signal interpretation based on wavelet packet transform for the detection of pile defects.
449 *Applied Sciences* **10**:2633.

450 **Schimmack M, Mercorelli P. 2018.** A wavelet packet tree denoising algorithm for images of
451 atomic-force microscopy. *Asian Journal of Control* **20**:1-12.

452 **Samaratunga D, Jha R, Gopalakrishnan S. 2016.** Wavelet spectral finite element for modeling
453 guided wave propagation and damage detection in stiffened composite panels. *Structural*
454 *Health Monitoring-an International Journal* **15**:317-334.

455 **Cruz FC, Simas Filho EF, Albuquerque MCS, Silva IC, Farias CTT, Gouvêa LL. 2016.**
456 Efficient feature selection for neural network based detection of flaws in steel welded joints
457 using ultrasound testing, *Ultrasonics* **73**:1-8.

458 **Wan P, Li QF. 2014.** Wavelet transform-based feature extraction for ultrasonic flaw signal
459 classification. *Neural Computing & Applications* **24**:817-826.

460 **Wang XK, Guan SY, Hua L, Wang B, He XM. 2019.** Classification of spot-welded joint strength
461 using ultrasonic signal time-frequency features and PSO-SVM method. *Ultrasonics* **91**:161-
462 169.

463 **Virmani J, Kumar V, Kalra N, Khandelwal N. 2013.** SVM-based characterization of liver ultra-
464 sound images using wavelet packet texture descriptors. *Journal of Digital Imaging* **26**:530-
465 543.

466 **Bagan H, Takeuchi W, Yamagata Y, Wang XH, Yasuoka Y. 2009.** Extended averaged learning
467 subspace method for hyperspectral data classification. *Sensors* **9**:4247-4270.

468 **Peng JW, Lv WH, Xing HY, Wu XJ. 2013.** Temperature compensation for humidity sensor
469   based on improved GA-BP neural network. *Chinese Journal of Scientific Instrument* **34**:153-
470   160.
471 **Han ZY, Huang XG. 2019.** GA-BP in thermal fatigue failure prediction of microelectronic chips.
472   *Electronics* **8**:542.
473 **Guo ZH, Wu J, Lu HY, Wang JZ. 2011.** A case study on a hybrid wind speed forecasting method
474   using BP neural network. *Knowledge-Based Systems* **24**:1048-1056.
475 **Garnier V, Chaix JF, Rossat M, Payan C, Corneloup G. 2009.** Non destructive characterisation
476   of concretes by ultrasonic wave's propagation. *Mecanique & Industries* **10**:299-303.
477 **Ren M, Zhang Q, Zhang J. 2019.** An introductory survey of probability density function control.
478   *Systems Science & Control Engineering* **7**:158-170.
479 **Shi YB, Zhang JJ, Jiao JJ, Zhao R, Cao HL. 2021.** Calibration analysis of high-G MEMS
480   accelerometer sensor based on wavelet and wavelet packet denoising. *Sensors* **21**:1231.
481 **Zhang G, Duffy AP, Orlandi A. 2017.** Statistical figures of merit for the feature selective
482   validation method. *IEEE Transactions on Electromagnetic Compatibility* 59:1482-1489.
483 **Javed AR, Usman M, Rehman SU, Khan MU, Haghighi MS. 2020.** Anomaly detection in
484   automated vehicles using multistage attention-based convolutional neural network. *IEEE*
485   *Transactions on Intelligent Transportation Systems* doi: 10.1109/TITS.2020.3025875.
486 **Mittal M, Iwendi C, Khan S, Javed AR. 2020.** Analysis of security and energy efficiency for
487   shortest route discovery in low-energy adaptive clustering hierarchy protocol using Levenberg-
488   Marquardt neural network and gated recurrent unit for intrusion detection system. *Transactions*
489   *on Emerging Telecommunications Technologies* doi: 10.1002/ett.3997.
490

Figure 1

Three-layer wavelet packet decomposition diagram.
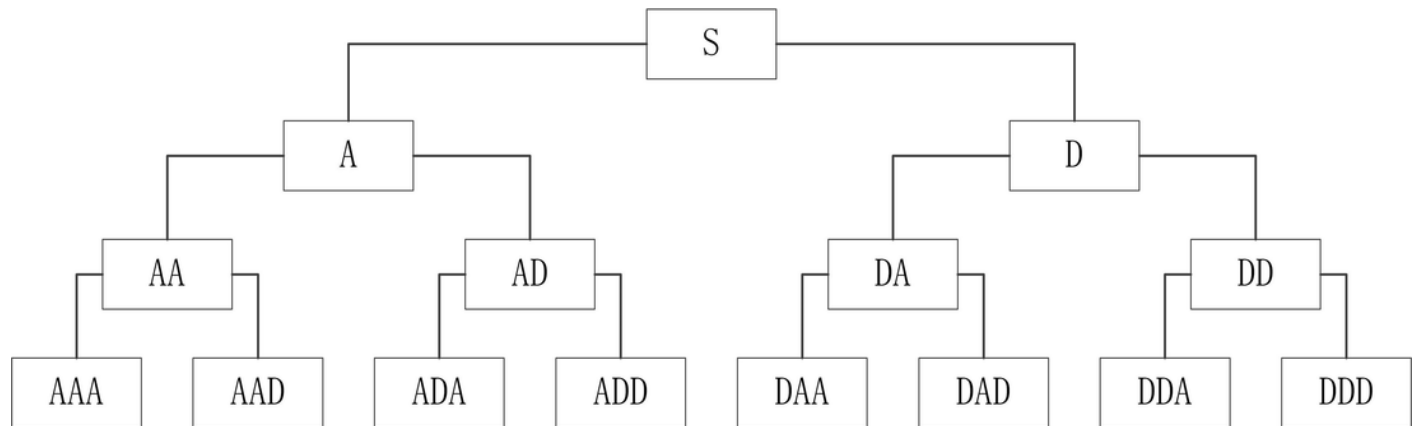
Figure 2

BP neural network structure
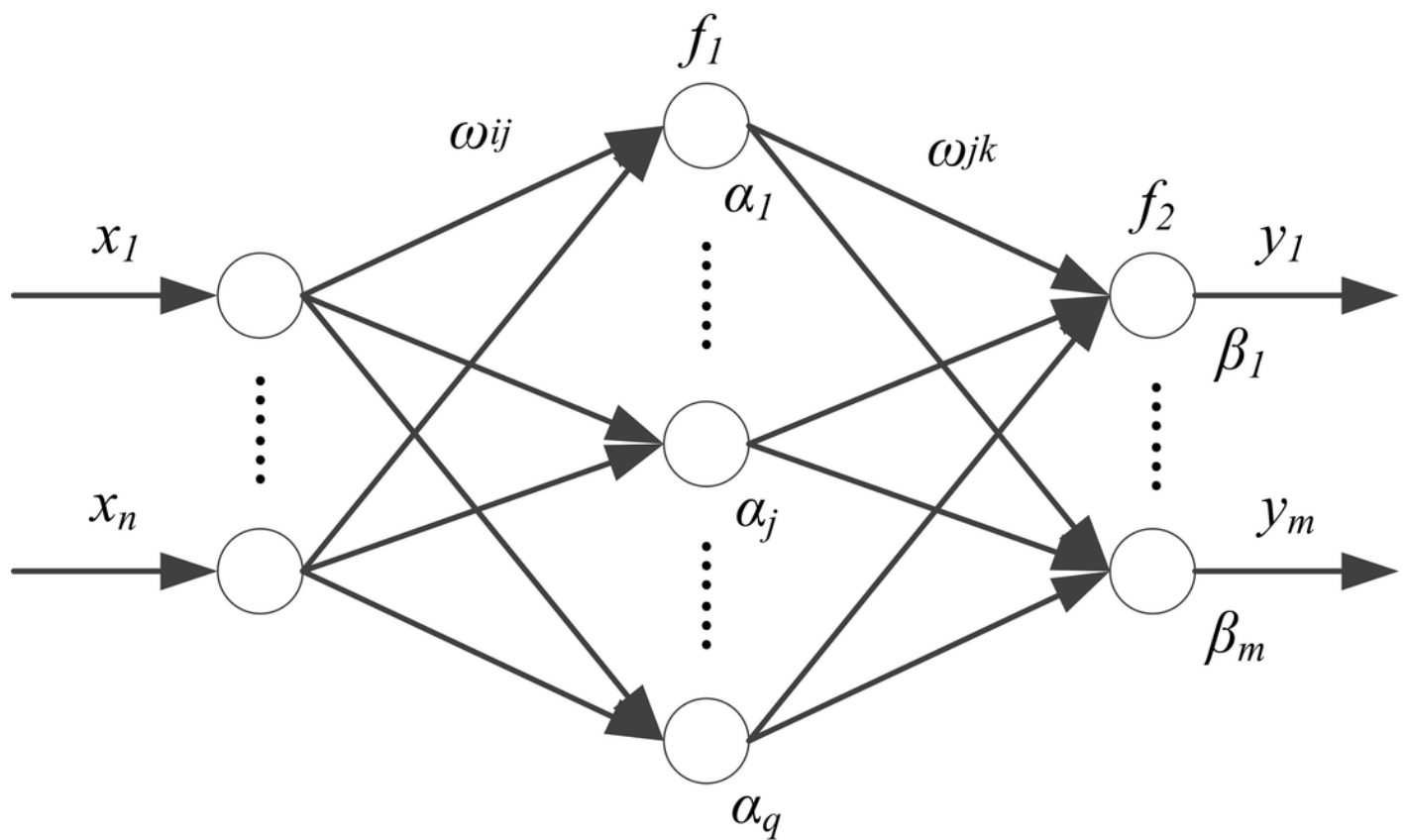
Figure 3

Parameters coding sequence

hidden layer nodes	ω_{ij}	α_j	ω_{jk}	β_m
q	$n\cdot(2^q-1)$	2^q-1	$(2^q-1)\cdot m$	m
binary coding		real coding		

Figure 4

algorithm flowchat
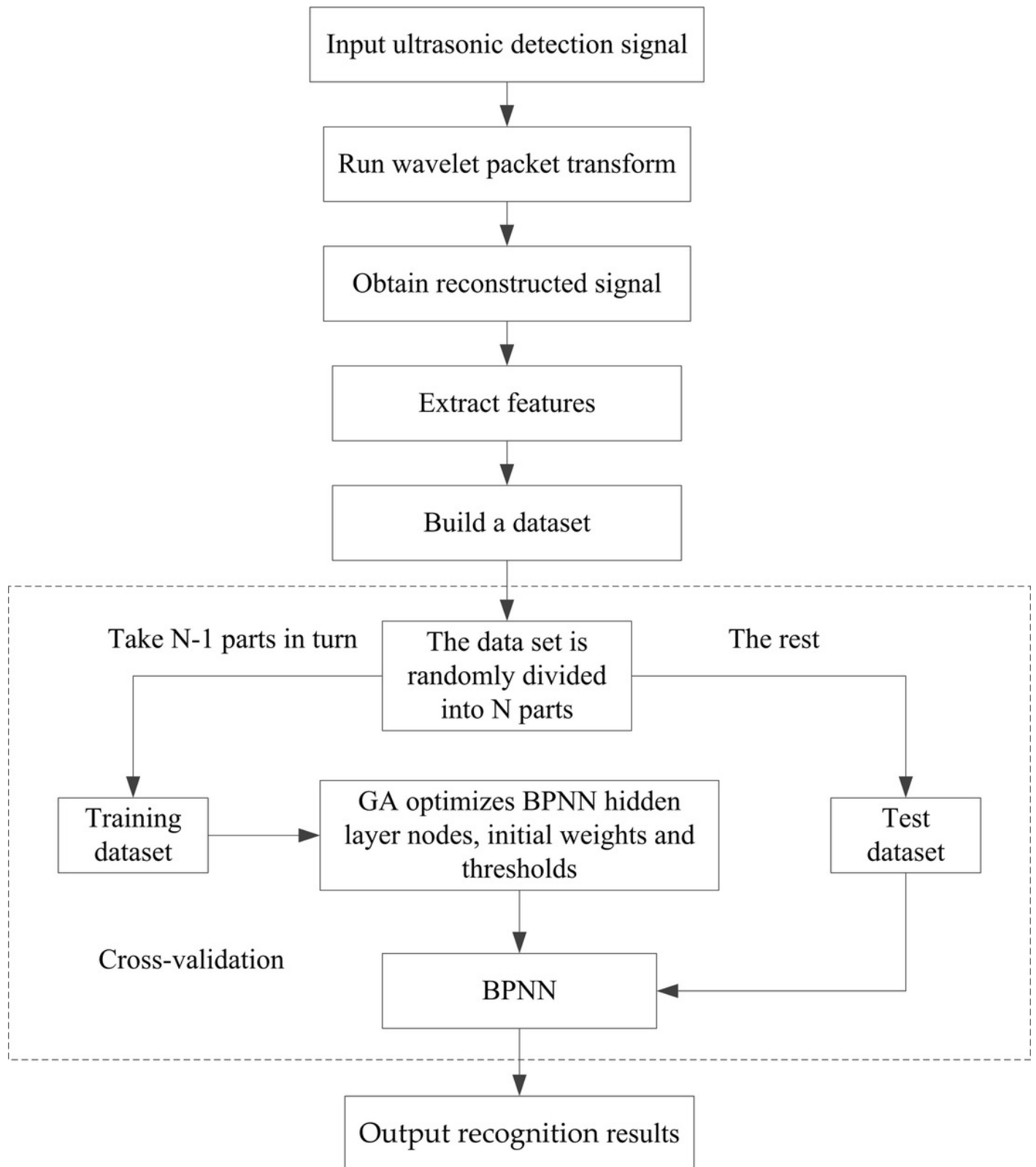
Figure 5

The schematic of the experimental setup for evaluating concrete defects with ultrasonic
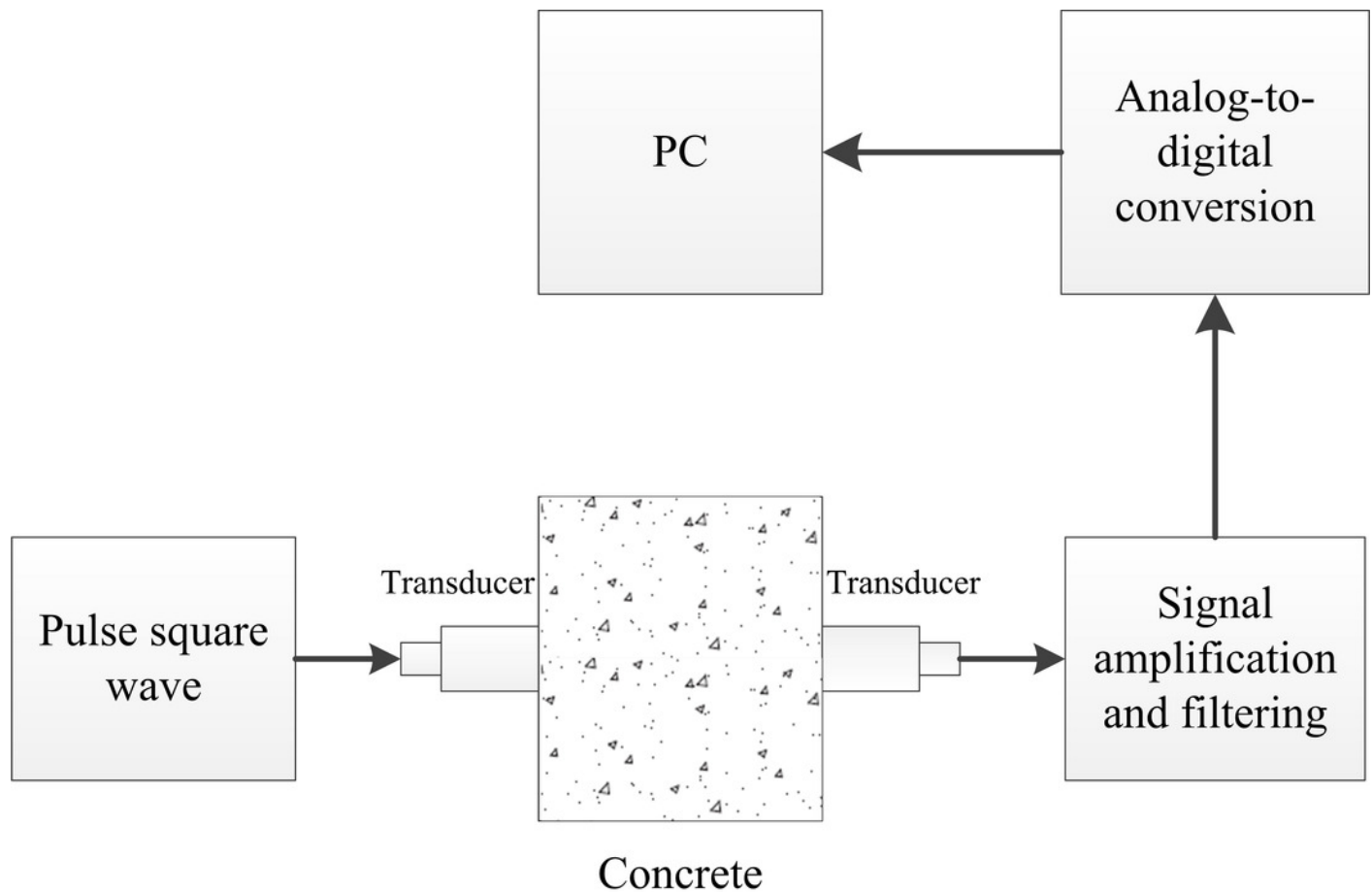
Figure 6

Concrete test block
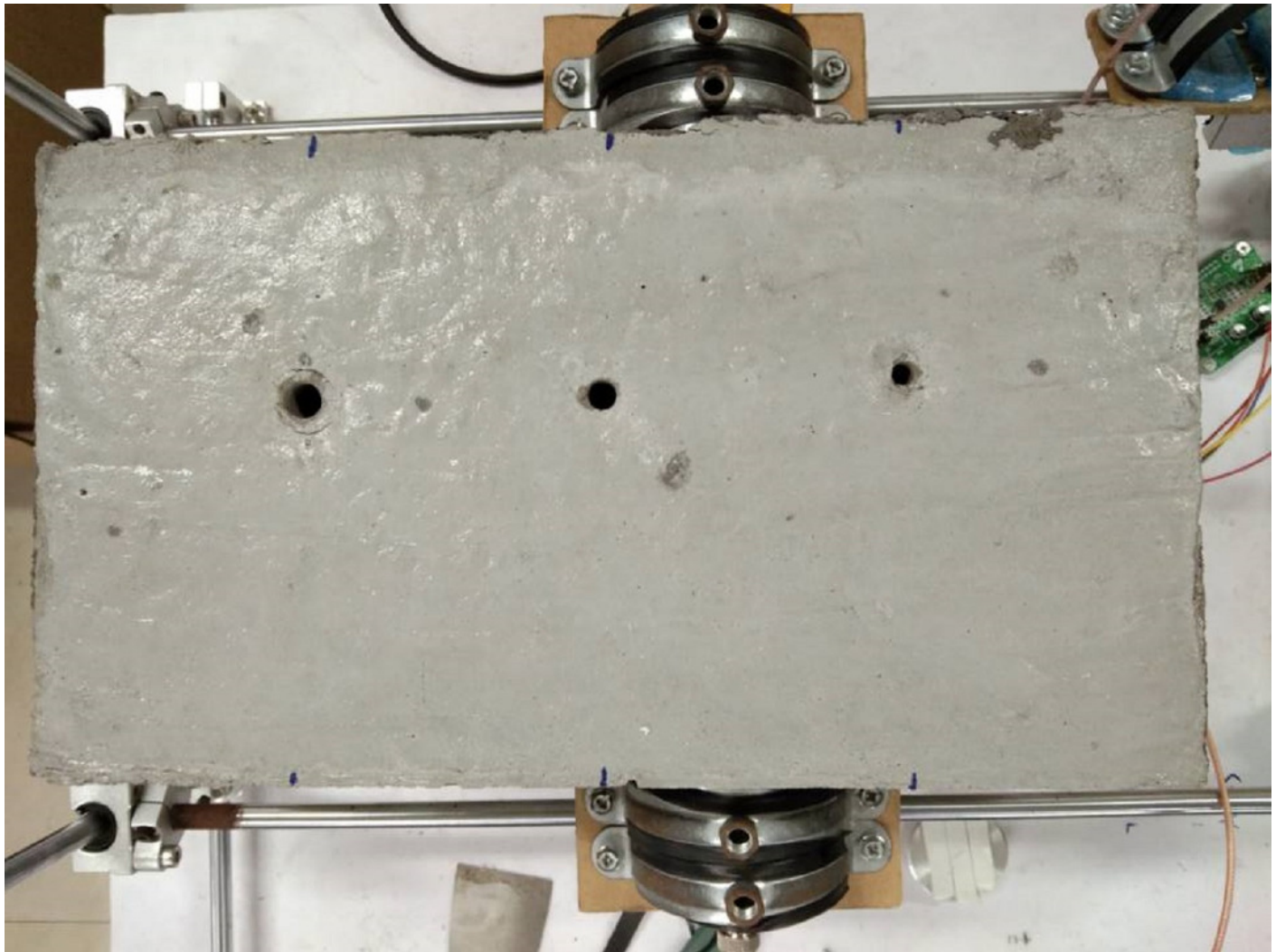
Figure 7

detection location diagram
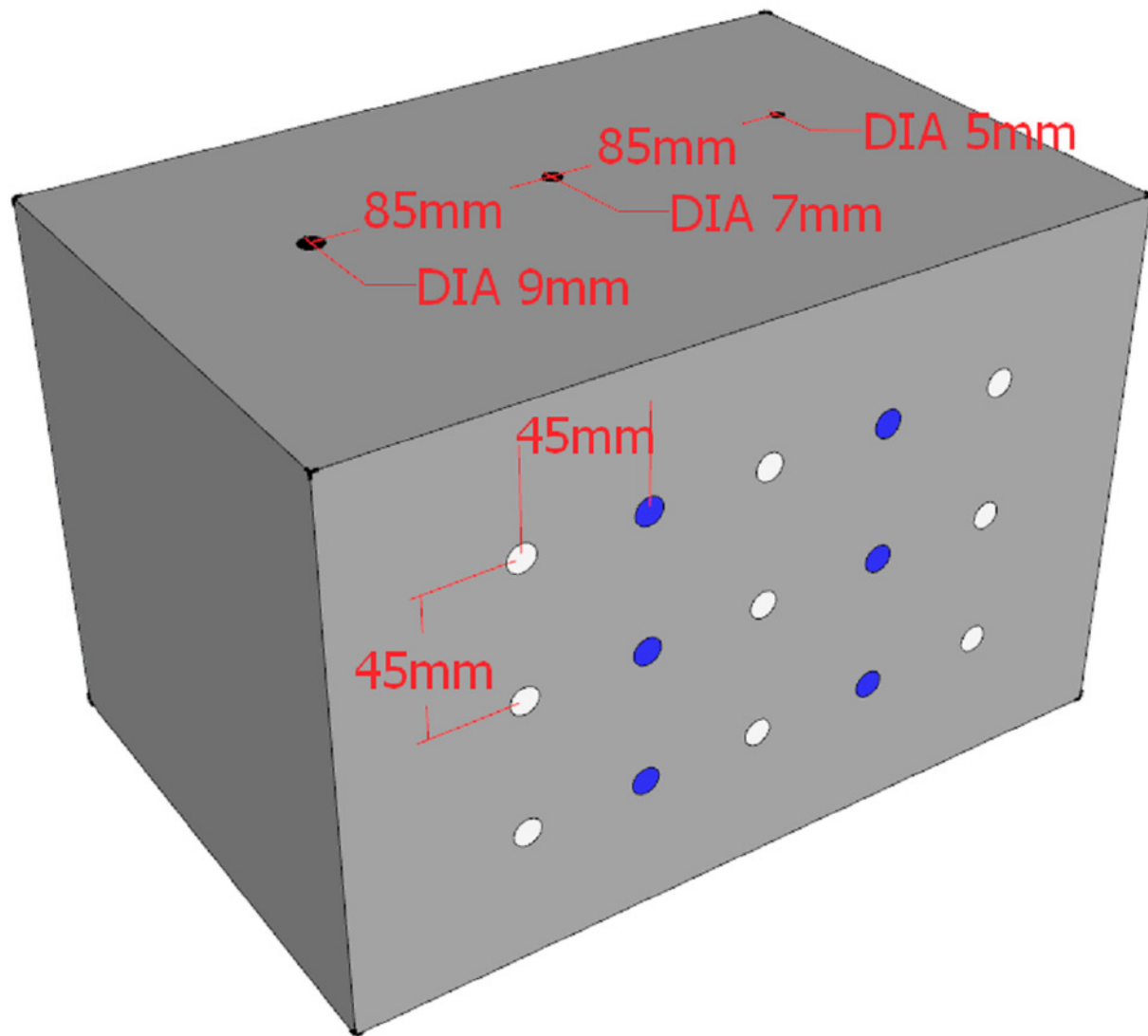
Figure 8

Diagram of the used experimental setup
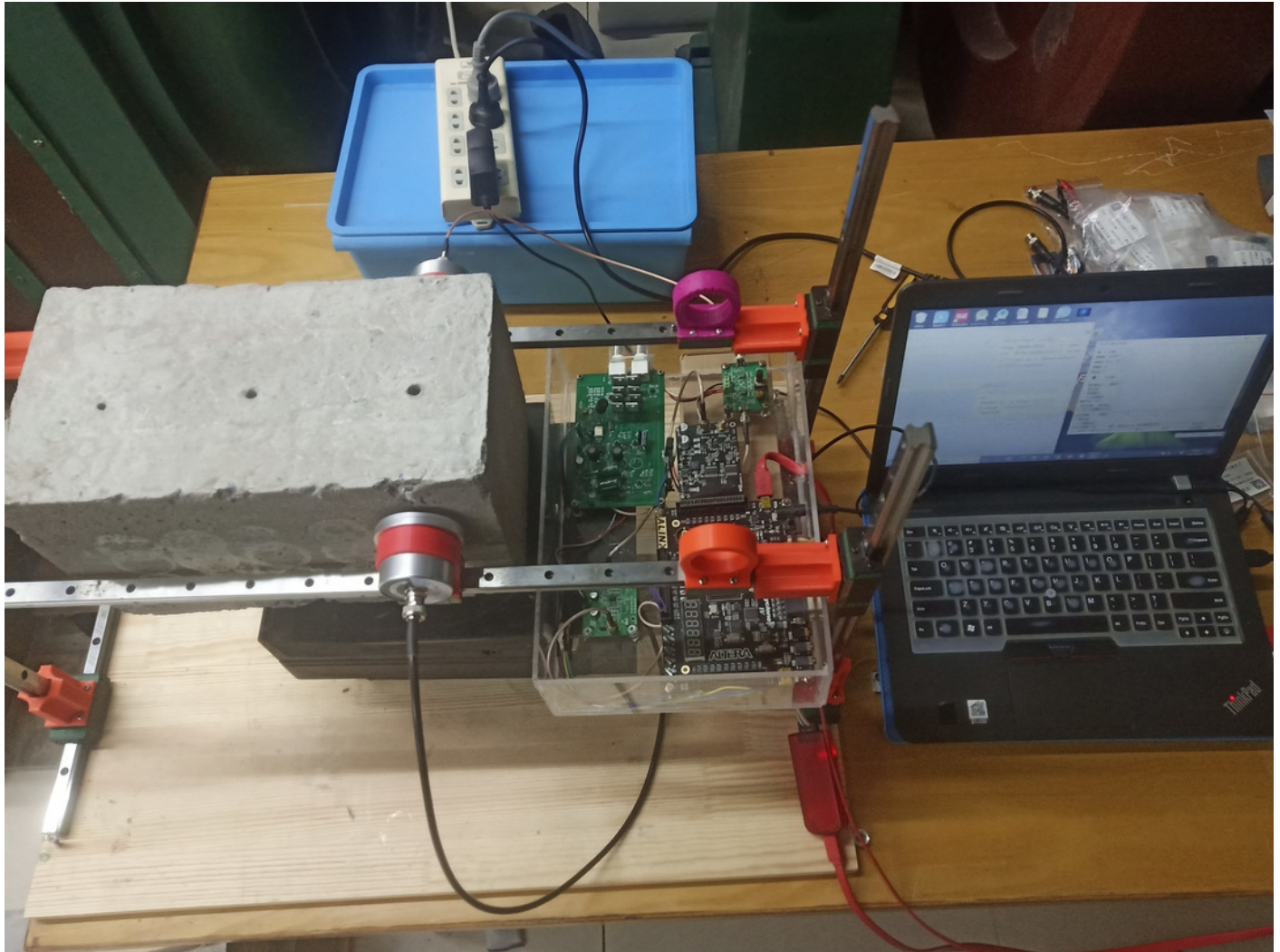
Figure 9

Four types of ultrasonic detection signal waveforms
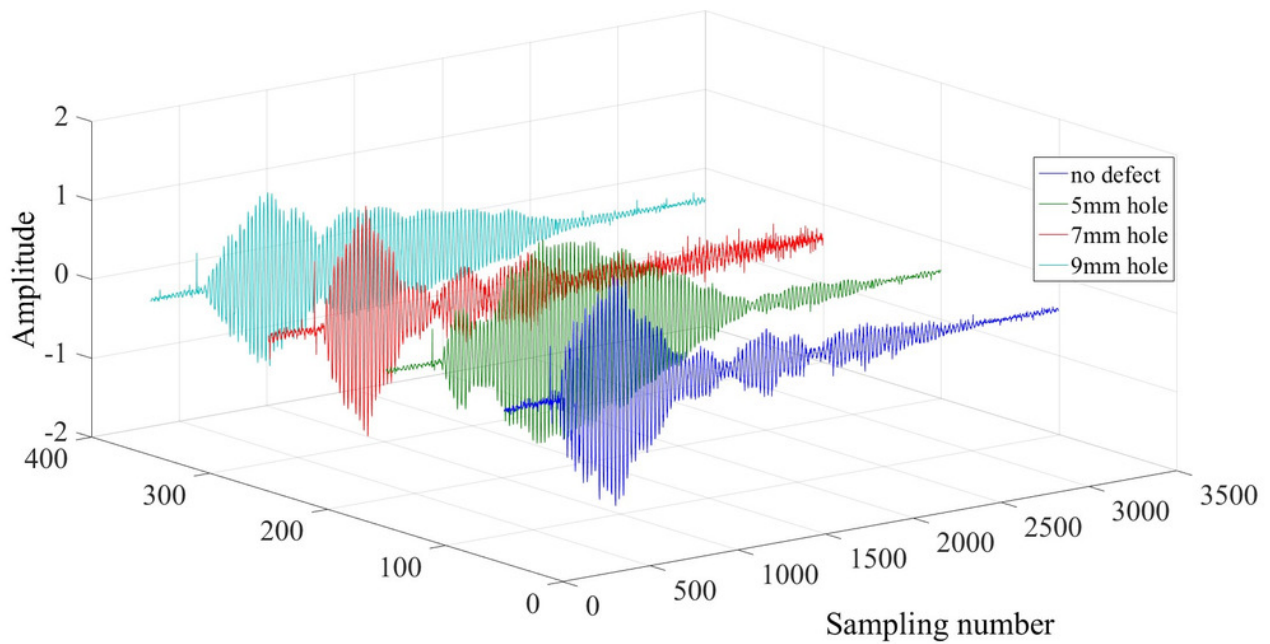
Figure 10

Mean distribution
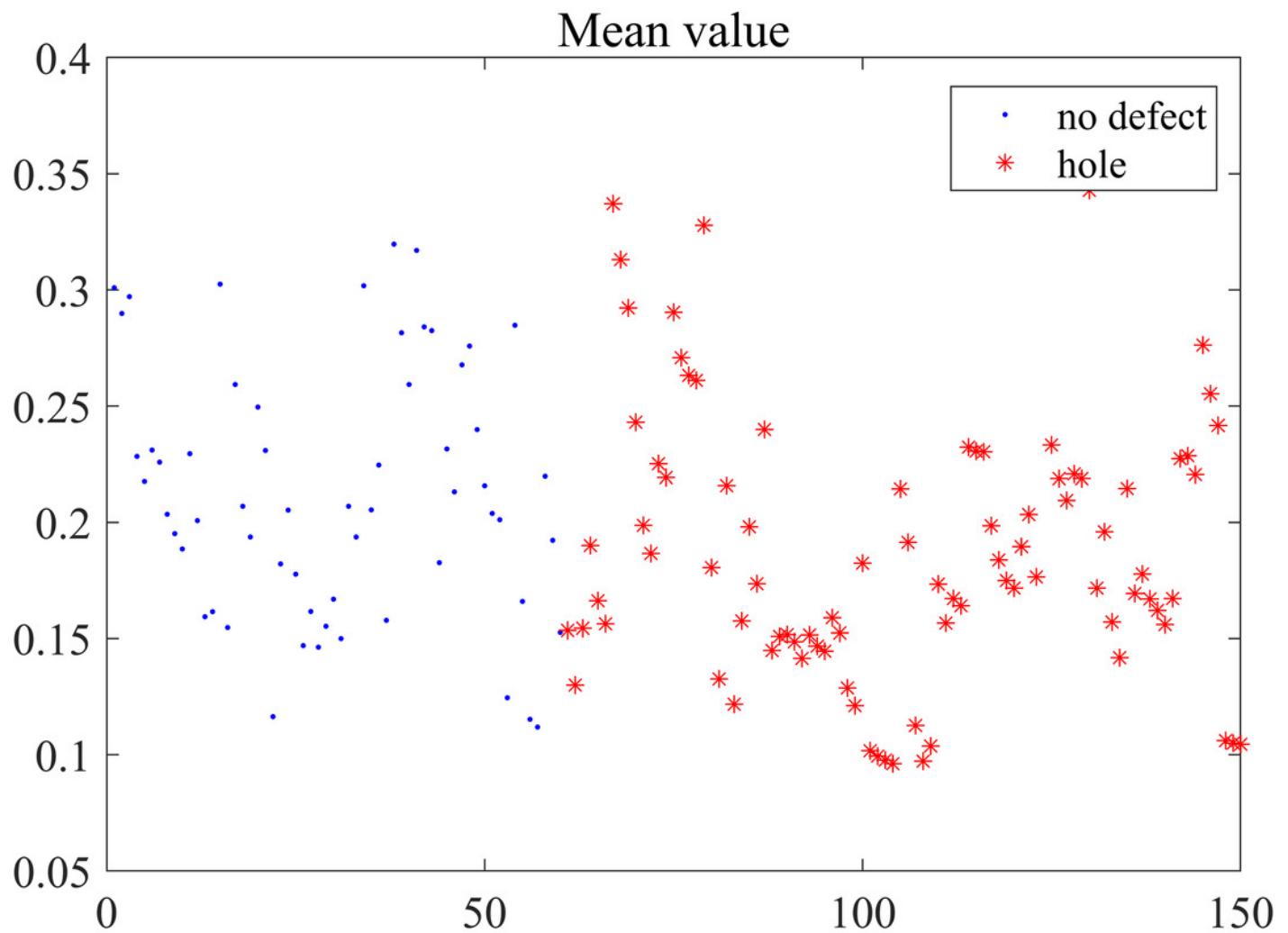
Figure 11

standard deviation distribution
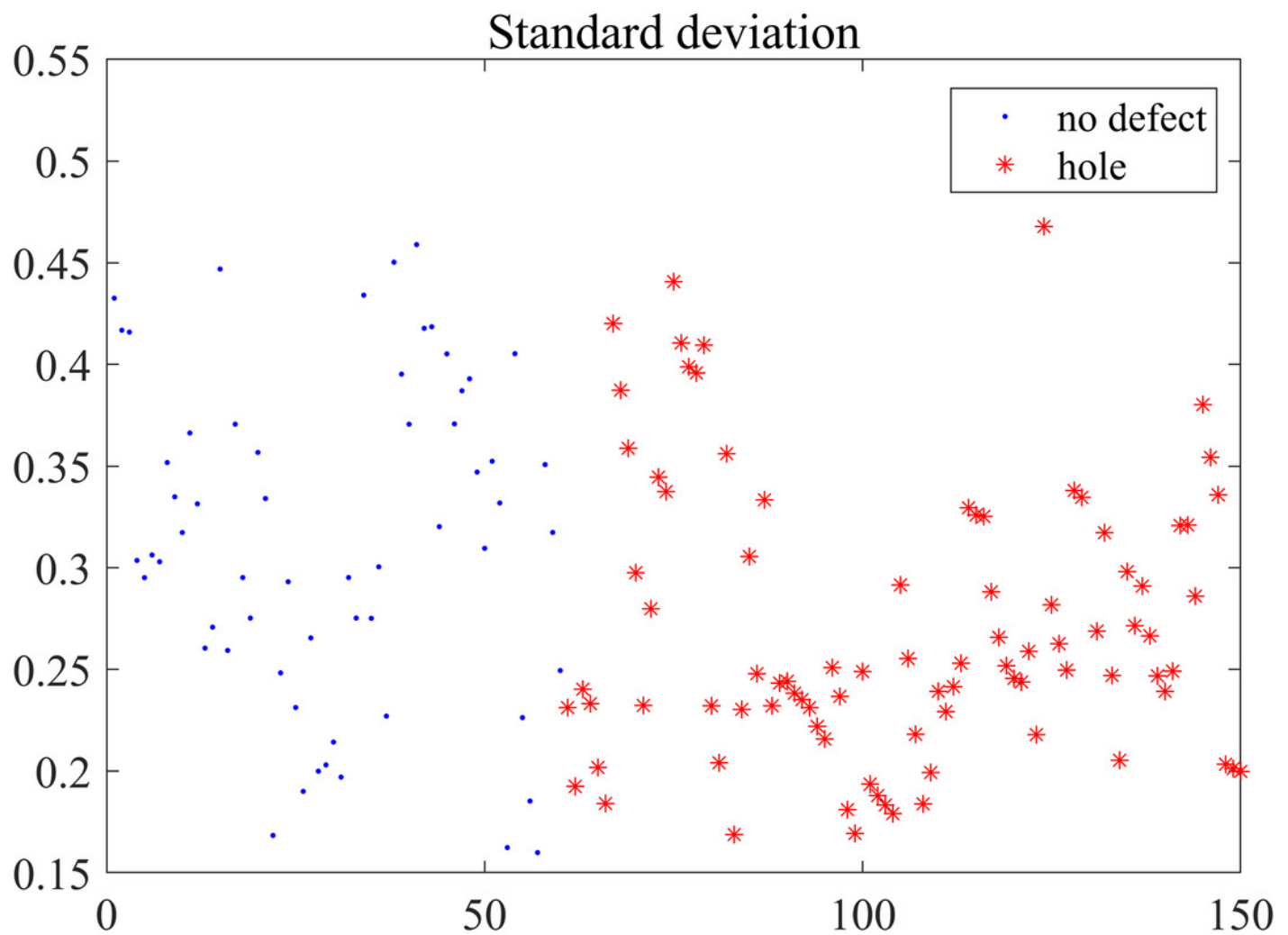
Figure 12

kurtosis coefficient distribution
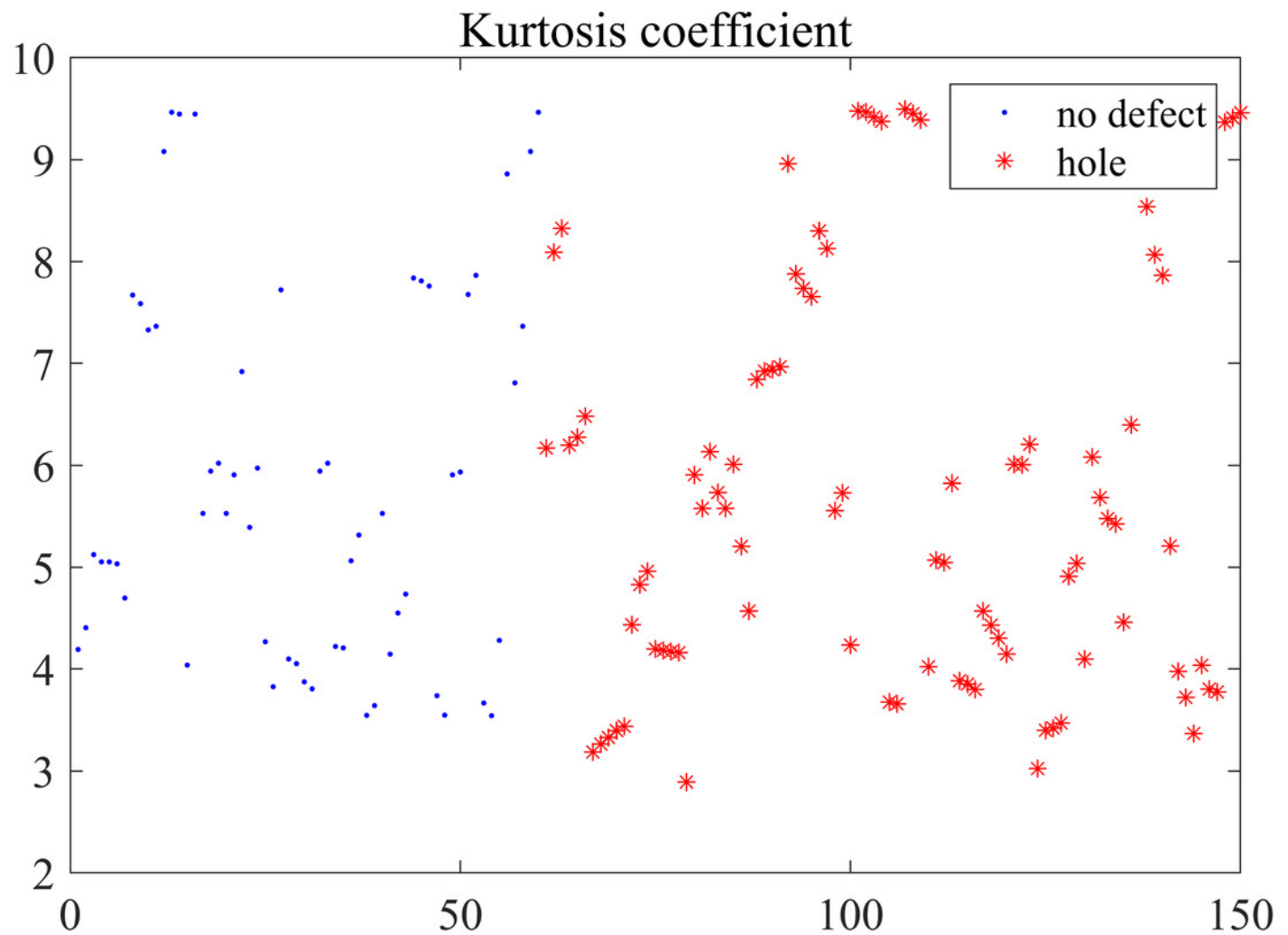
Figure 13

skewness coefficient distribution
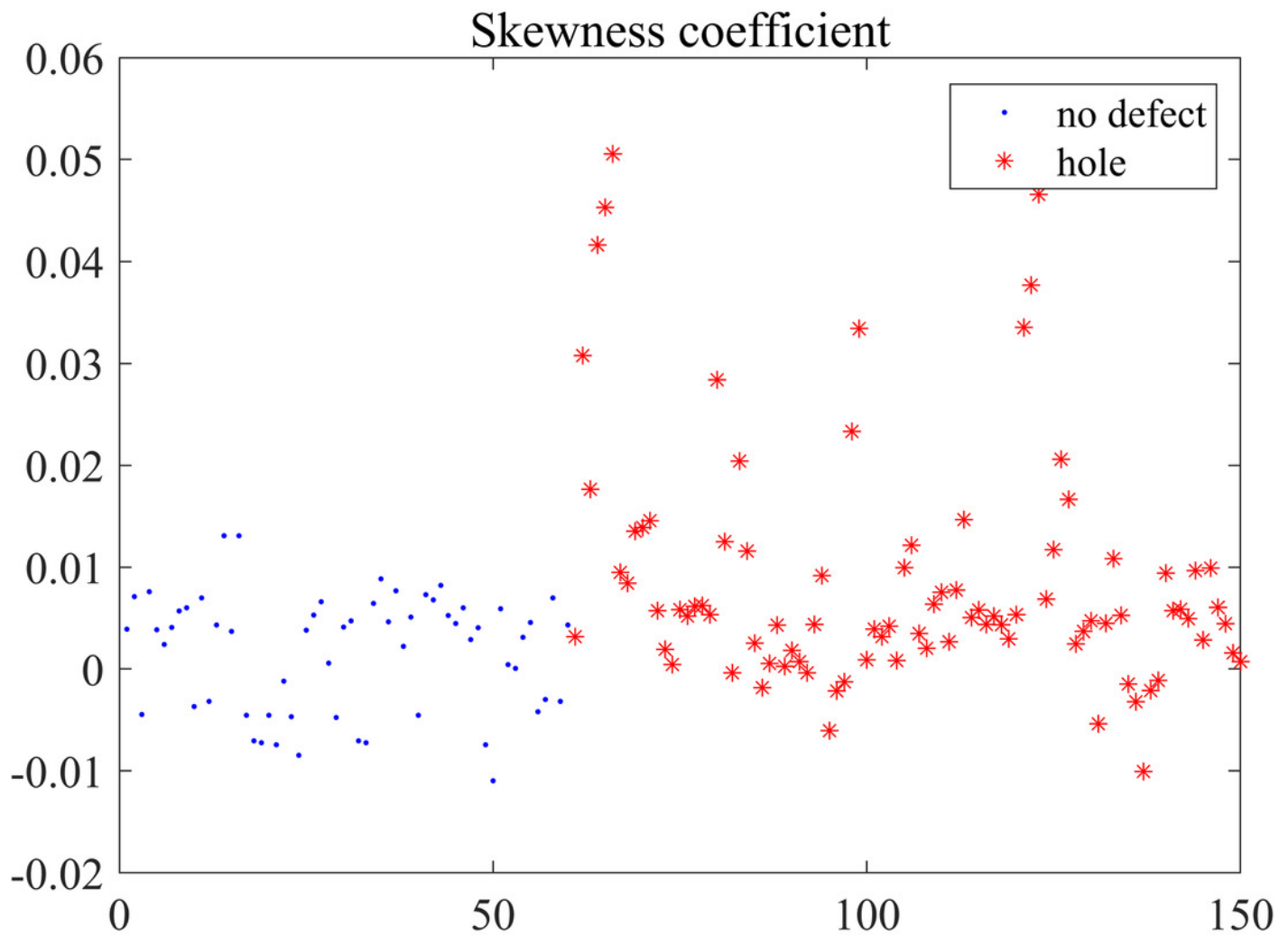
Figure 14

energy ratio distribution
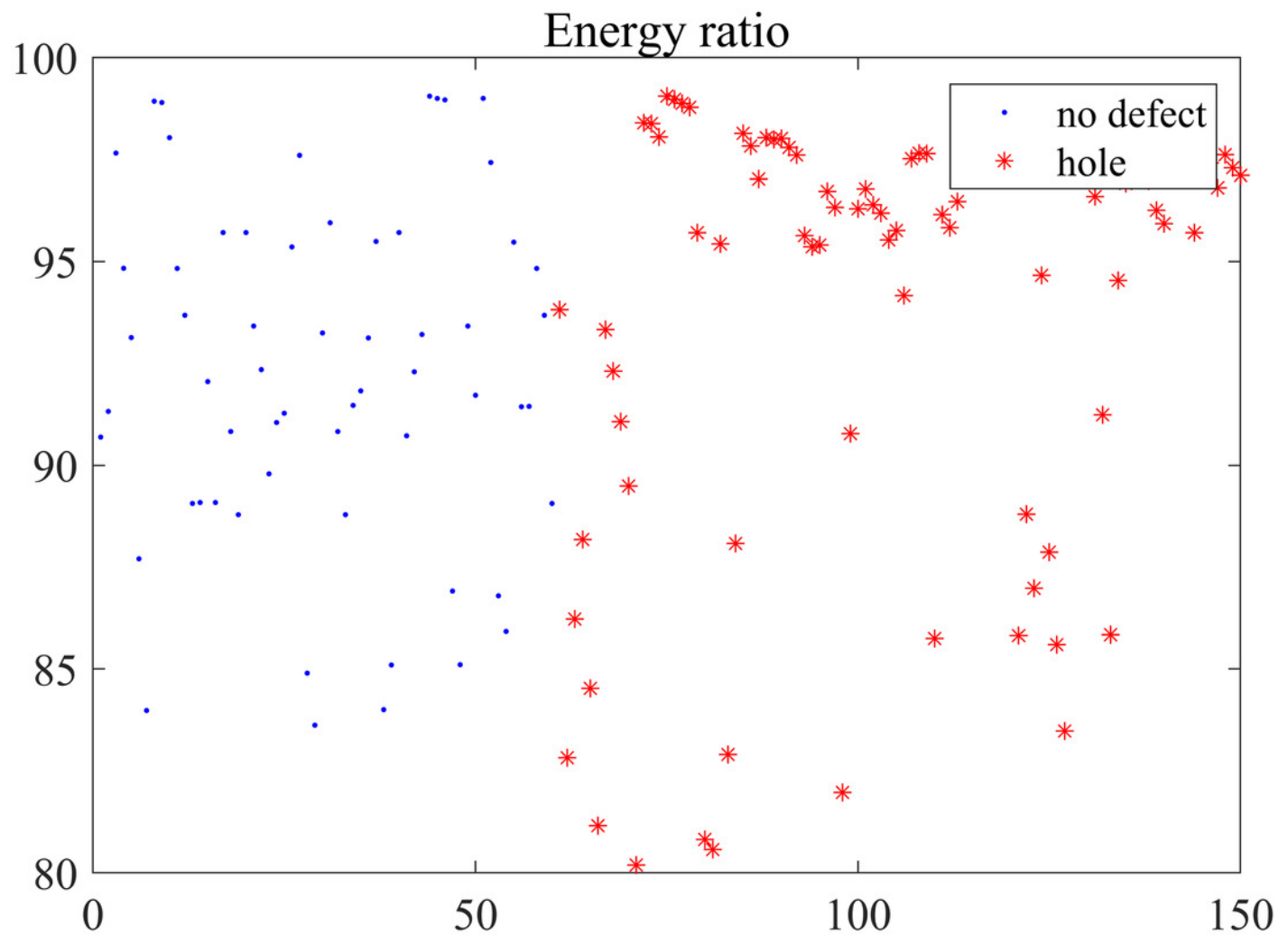
Figure 15

The error curves in training dataset
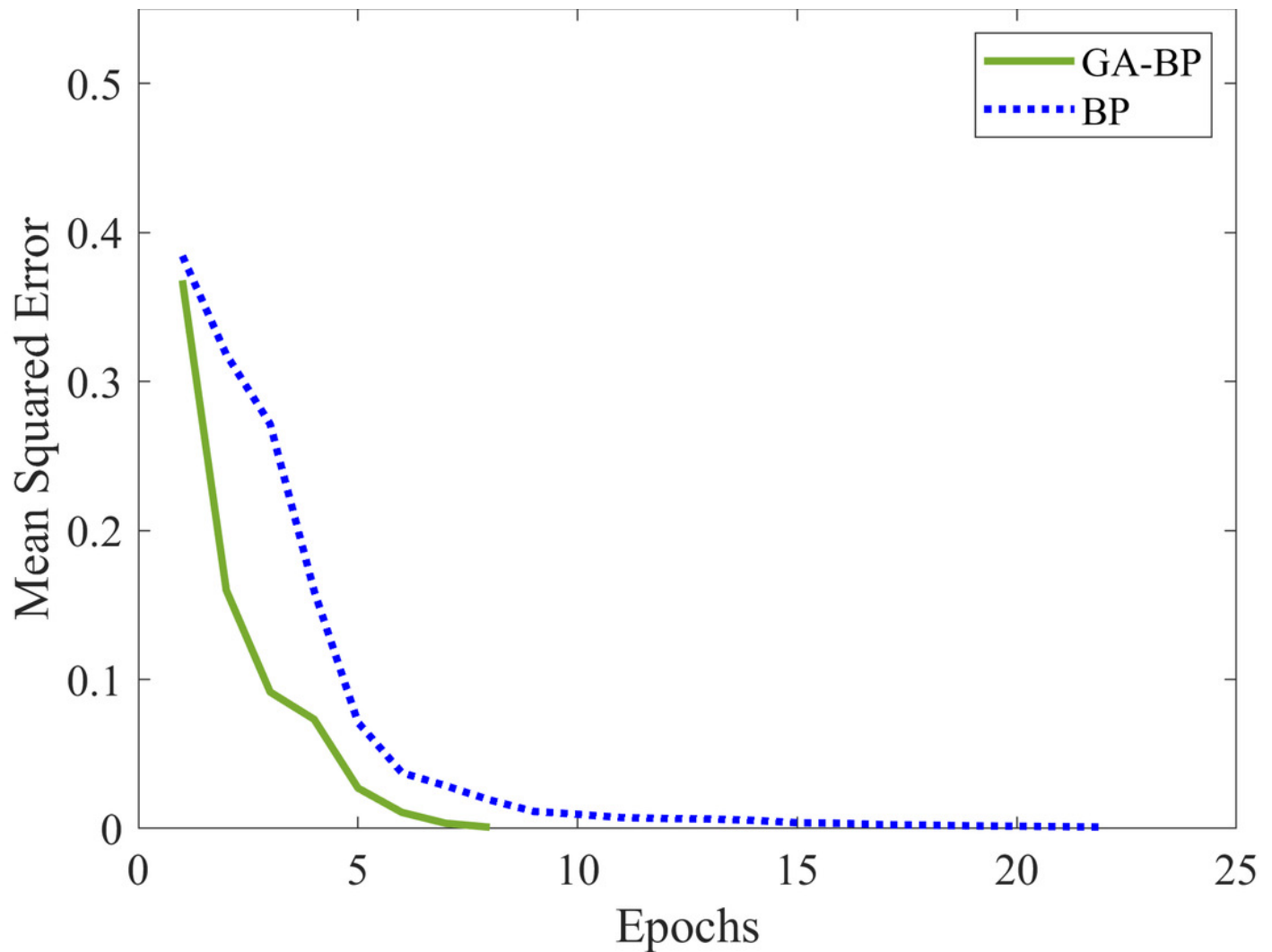
Figure 16

The error curves in test dataset
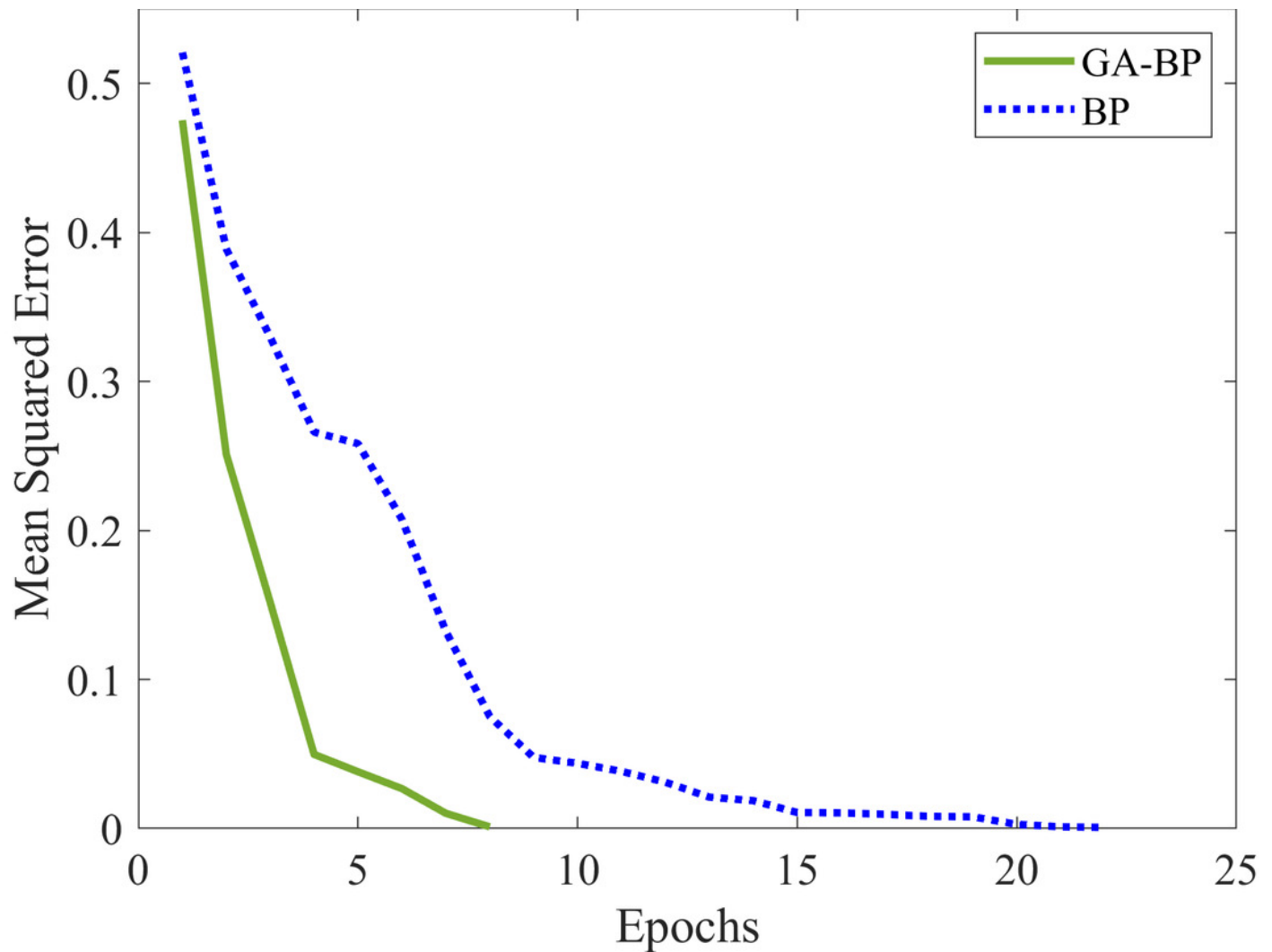
Training dataset recognition results

Table 1 Training dataset recognition results.

No.	Class		Recognition result		Accuracy(%)	Average Accuracy(%)
			True	False		
1	No defect		38	2	96	
	Defect	5mm 7mm 9mm	58	2		
2	No defect		36	4	95	95.33
	Defect	5mm 7mm 9mm	59	1		
3	No defect		37	3	95	
	Defect	5mm 7mm 9mm	58	2		

Test dataset recognition results

Table 2 Test dataset recognition results.

No.	Class		Recognition result		Accuracy(%)	Average Accuracy(%)
			True	False		
1	No defect		19	1	92	
	Defect	5mm				
		7mm	27	3		
		9mm				
2	No defect		18	2	90	91.33
	Defect	5mm				
		7mm	27	3		
		9mm				
3	No defect		20	0	92	
	Defect	5mm				
		7mm	26	4		
		9mm				

Comparison of results of 4 different methods

Table 3 Comparison of results of 4 different methods.

Model	Class	Sample number	Average accuracy(%)
RBF	No defect/Hole	150	86
SVM	No defect/Hole	150	87.33
BPNN	No defect/Hole	150	86.67
GA-BPNN	No defect/Hole	150	91.33